Trans. Korean Soc. Noise Vib. Eng., 26(2) : 157~164, 2016
http://dx.doi.org/10.5050/KSNVE.2016.26.2.157

한국소음진동공학회논문집 제 26 권 제 2 호, pp. 157~164, 2016
ISSN 1598-2785(Print), ISSN 2287-5476(Online)

A Study on Vibration Control Performance of Macpherson Type Semi-Active Suspension System

맥퍼슨 타입 반 능동 현가장치의 진동제어 성능 고찰

Saikat Dutta*, Chulhee Han*, TaeHoon Lee* and Seung-Bok Choi†

사이카 두타 · 한 철 희 · 이 태 훈 · 최 승 복

(Received December 8, 2015 ; Revised January 18, 2016 ; Accepted January 18, 2016)

Key Words : Adaptive Moving Sliding Model Control(적응 움직임 슬라이딩모드 제어), Macphersen Type Vehicle Suspension(맥퍼슨 타입 현가장치), Vibration Control(진동제어), MR Damper(MR 댐퍼)

ABSTRACT

The paper studies a comparison analysis of semi-active control strategies for a Macpherson strut type suspension system consisting of MR(magneto-rheological) damper. As a first step, in order to formulate governing, a dynamic full model of a Macpherson strut is developed considering the kinematics. The nonlinear equation of motion of the strut is then linearized around the equilibrium point. A new adaptive moving sliding model controller is developed for fast response of the system. A newly proposed adaptive moving sliding mode control strategy is then compared with conventional sliding mode controller and skyhook controller. The comparison is made for two different types of road inputs; bump and random road profiles showing superior vibration control performance in time and frequency domains.

요 약

이 논문은 MR 댐퍼를 적용한 맥퍼슨 타입의 반 능동 현가장치의 진동제어에 관한 연구를 보여준다. 맥퍼슨 스트럿의 기하학적 분석을 바탕으로 동역학 지배 방정식이 설립되었으며, 제어기 설계를 위해 평형 점 근처의 비선형적 운동이 선형화하였다. 이어서 시스템의 향상된 반응시간을 위해 새로운 적응 움직임 슬라이딩모드 제어기를 제안하였으며, 시뮬레이션을 통해 범프와 랜덤도로에서 차량으로 가해지는 진동에 따른 제어 성능을 기존슬라이딩모드 제어기 및 스카이훅 제어기와의 비교를 통해 우수성을 평가하였다.

1. Introduction

Application of semi-active suspension systems in vehicles to suppress the unwanted vibration level has increased significantly with the advances of smart fluids. By using Magneto-rheological fluid damper as controllable damper, suspension performances are improved by a good amount. Because of its ability to achieve a wide range of

† Corresponding Author ; Member, Mechanical Engineering of Inha University
E-mail: seungbok@inha.ac.kr
* Mechanical Engineering of Inha University

‡ Recommended by Editor Il Kwon Oh

viscosity by varying applied magnetic field, various semi-active control logics are developed to obtain good performance of the system. Karnopp et al.[1] first developed "skyhook" damper control algorithm for a vehicle suspension system and show that this provide better performance. Ahmedian et al.[2] studied ground-hook and hybrid control strategies for MR suspensions for quarter car models. Choi et al.[3] developed a cylindrical MR damper and studied its practical feasibility through the road test evalution.

Most of the researchers considered the model as quarter car models which is not exactly same in the practical case. The Macpherson strut type suspensions are widely mostly used in light or medium sized vehicles The kinematic and dynamic analysis of the Macpherson strut suspension is carried out by Fallah[4], Hurel[5] etc. The detailed analysis of Macpherson strut with MR dampers are not studied much. Hong et al.[6] proposed a new MacPherson strut model where the unsprung and sprung mass were considered as point masses and the rigid body rotations were ignored. Andersen[7] developed a dynamic model of Macpherson strut system using Lagrange multiplier for the constrained equations and presented a system of algebraic equations. The accurate modeling of the Macpherson strut is needed to get the important parameters like camber angle, track alteration etc. which governs the stability of the vehicle.

The main contribution of this work is to develop a new robust controller to control the motions of Macpherson strut which is integrated with MR damper. Firstly, the Macpherson strut type suspension system with MR damper is modeled considering the dynamic and kinematic relationships. The nonlinear equation of motion is then linearized about the equilibrium point to make it suitable for semi-active control algorithm. A new adaptive moving sliding mode controller is developed which is shown to perform much better. The proposed algorithm is evaluated at bump and random road conditions and compared with existing controllers.

2. Model of Macpherson Strut Suspension

The schematic diagram of Macpherson suspension system is shown in Fig. 1. During equilibrium, the point A was at A_0 making an angle θ_0 with Y-axis at Fig. 2. At equilibrium position, the origin of the coordinate system O coincides with B. The control arms rotates at angle θ which is measured counter clock-wise and the sprung mass moves by an amount z_s. The displacement of the points on the spindle-wheel assembly can be formulated as follows[4]:

$$\begin{bmatrix} y_C & y_E & y_P \\ z_C & z_E & z_P \\ 1 & 1 & 1 \end{bmatrix} = \begin{bmatrix} a_{11} & a_{12} & y_A-(a_{11}y_{A0}+a_{12}z_{A0}) \\ a_{21} & a_{22} & z_A-(a_{21}y_{A0}+a_{22}z_{A0}) \\ 0 & 0 & 1 \end{bmatrix} \begin{bmatrix} y_{C0} & y_{E0} & y_{P0} \\ z_{C0} & Z_{E0} & z_{P0} \\ 1 & 1 & 1 \end{bmatrix} \quad (1)$$

The coefficients, $a_{11}=a_{22}=\cos\varphi$ and $a_{12}=-a_{21}=\sin\varphi$, where φ is the wheel rotation about x-axis or the camber angle. The equation can be reduced by considering $a_{11}=a_{22}=1$ and $a_{12}=-a_{21}=\varphi$ as follows:

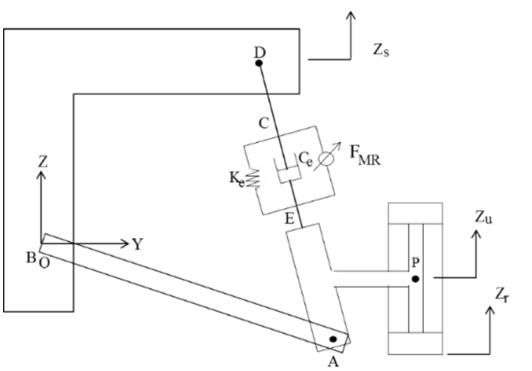

Fig. 1 Schematic diagram of Macpherson suspension system

$$y_c = y_{c0} + \varphi z_{c0} + y_A - (y_{A0} + \varphi z_{A0}) \\ = a_C + b_C\varphi + y_A,\ z_C = -\varphi a_C + b_C + z_A \quad (2)$$

where the coefficients are obtained from the following equilibrium coordinates as $a_C = u_{C0} - y_{A0}$ and $b_C = z_{C0} - z_{A0}$. Similarly y_E, y_P, z_E and z_P can be also be written in terms of a_E, b_E, a_P and b_P. The constraints of the strut can be found as

$$\tan\alpha = \frac{y_C - y_E}{z_C - z_E} = \frac{y_A - y_D}{z_A - z_D} \quad (3)$$

The coordinate (y_A, z_A) can be obtained from the rotation of the control arm and the constrained equations of the control arm are given by

$$y_A = L_2\cos(\theta_0 + \theta), \\ z_A = L_2\sin(\theta_0 + \theta) + z_S \quad (4)$$

where, L_2 is the length of the control arm and θ_0 is the initial angle of the control arm. The above equations can be linearized considering the angle θ small as follows:

$$y_A = L_2\cos\theta_0\cos\theta - L_2\sin\theta_0\sin\theta \\ = L_C - L_S\theta \quad (5)$$

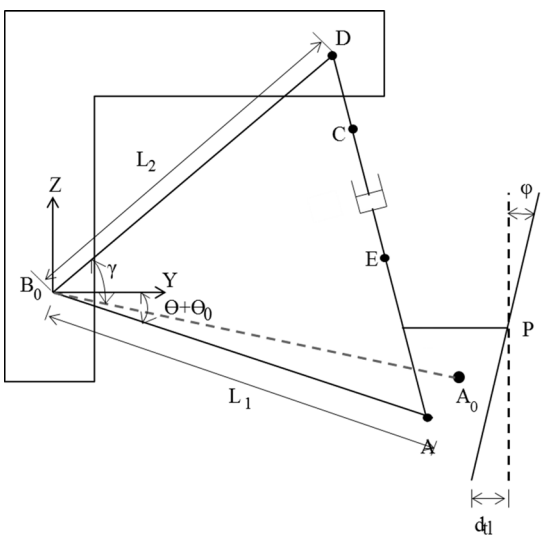

Fig. 2 The position of the key points and corresponding equilibrium position

$$z_A = L_2\sin\theta_0\cos\theta + L_2\cos\theta_0\sin\theta + z_S \\ = L_S - L_C\theta + z_S \quad (6)$$

where, $L_C = L_2\cos\theta_0$ and $L_S = L_2\sin\theta_0$.

Substitution of the values of equations (5) and (6) in equation (3) yields the following equation.

$$\frac{a_C + b_C\varphi - a_E - b_E\varphi}{-\varphi a_C = b_C + \varphi a_E - b_E} = \frac{L_C - L_S\theta - y_{D0}}{L_S - L_C\theta - z_{D0}} \quad (7)$$

Neglecting the higher order terms of θ, Eq. (7) leads to the follow equation.

$$\varphi = P_1 + P_2\theta + P_3\theta^2 \quad (8)$$

where,

$$P_1 = \frac{Q_1}{Q_3},\ P_2 = \frac{Q_1}{Q_3}\left(\frac{Q_2}{Q_1} - \frac{Q_4}{Q_3}\right) \text{ and}$$

$$P_3 = -\frac{Q_1 Q_4}{Q_3^2}\left(\frac{Q_2}{Q_1} - \frac{Q_4}{Q_3}\right).$$

$$Q_1 = b_{CE}(L_C - y_{D0}) - a_{CE}(L_S - z_{D0}),$$

$$Q_2 = -(a_{CE}L_C + b_{CE}L_S),$$

$$Q_3 = b_{CE}(L_s - z_{D0}) - a_{CE}(L_C - y_{D0}) \text{ and}$$

$$Q_4 = b_{CE}L_C - a_{CE}L_S,$$

$$a_{CE} = a_C - a_E \text{ and } b_{CE} = b_C - b_E.$$

Now, the unknowns (y_P, z_P) can be calculated as

$$y_P = a_P + b_P\varphi + y_A \\ = a_P + b_P(P_1 + P_2\theta + P_3\theta^2) + L_C - L_S\theta \quad (9) \\ = P_4 + P_5\theta + P_6\theta^2$$

$$z_P = -\varphi a_C + b_C + z_A \\ = -a_P(P_1 + P_2\theta + P_3\theta^2) + b_P + L_S - L_C\theta + z_S \\ = P_7 + P_8\theta + P_9\theta^2 + Z_S \quad (10)$$

where,

$$P_4 = a_P + L_C + b_P P_1,$$

$$P_5 = b_P P_2 - L_S \text{ and } P_6 = b_P P_3$$

$$P_7 = -a_P P_1 + L_S + b_P,$$

$$P_9 = -a_P P_2 - L_C \text{ and } P_9 = -a_P P_3.$$

The deflection of the spring, ΔL is given by

$$\Delta L = L_3 - L_3' \tag{11}$$

where L_3 is the length of the spring at equilibrium position and L_3' is the instantaneous length of spring. From geometry neglecting the highest order terms of θ, the deflection of the spring equation is obtained as,

$$\Delta L = -\frac{K_D}{2L_3}\theta, \text{ where } K_D = 2L_1L_2\sin\gamma \tag{12}$$

In the above, the γ is the angle between the control arm and the line joining points B and D. Tire lateral tire deflection is computed as follows:

$$d_{tl} = y_u - \varphi R = R_1 + R_2\theta + R_3\theta^2 \tag{13}$$

where, R is tire effective radius given by

$$R_1 = P_4 - P_1R, \quad R_2 = P_5 - P_2R, \quad R_3 = P_6 - P_3R.$$

The equation of motion of the Macpherson strut with MR damper can be obtained using Lagrange's method as follows:

$$\begin{aligned}
\ddot{z}_s &= F_1(z_s, \dot{z}_s, \theta, \dot{\theta}, z_r, \dot{z}_r, F_{MR}, u)\\
\ddot{\theta} &= F_2(z_s, \dot{z}_s, \theta, \dot{\theta}, z_r, \dot{z}_r, F_{MR}, u)\\
\dot{F}_M &= F_3(z_s, \dot{z}_s, \theta, \dot{\theta}, z_r, \dot{z}_r, F_{MR}, u)
\end{aligned} \tag{14}$$

In the above, the dynamics of the MR damper can be expressed as the following equation,

$$\dot{F}_M = -\frac{1}{\tau}F_M + \frac{1}{\tau}u. \tag{15}$$

where, τ is the time constant of the MR damper.

Now, we consider the state variables as $[x_1, x_2, x_3, x_4, x_5]^T = [z_s, \dot{z}_s, \theta, \dot{\theta}, F_M]^T$. The above equations of motion is highly nonlinear. For further work and to incorporate control strategies for the system, the system of equations should be linearized at the equilibrium position as follows:

$$\dot{x} = Ax + Dz_r + Bu,\ x_0 = 0. \tag{16}$$

where,

$$A = \frac{1}{A_D}\begin{bmatrix} 0 & D & 0 & 0 & 0\\ a_{21} & a_{22} & a_{23} & a_{24} & a_{25}\\ 0 & 0 & 0 & D & 0\\ a_{41} & a_{42} & a_{43} & a_{44} & a_{45}\\ 0 & 0 & 0 & 0 & a_{55} \end{bmatrix}$$

$$A_D = m_u^2M_2^2 - M_1(m_s + m_u),$$

$$a_{21} = -K_tm_uM_2^2 + K_tM_1,$$

$$a_{22} = -C_tm_uM_2^2 + C_tM_1,$$

$$a_{23} = M_1(P_8 + P_9\theta)K_t - M_2m_u\left(R_4K_{tl} + M_2^2K_t + \frac{K_SK_D^2}{4L^2}\right),$$

$$a_{24} = M_1M_2C_t - M_2m_u\left(M_2^2C_t + \frac{C_SK_D^2}{4L^2}\right),$$

$$a_{25} = \frac{M_2K_Dm_u}{2L_S},$$

$$a_{41} = K_tM_2(m_s + m_u) - K_tM_2m_u,$$

$$a_{42} = C_tM_2(m_s + m_u) - C_tM_2m_u,$$

$$a_{43} = -M_2(P_8 + P_9\theta)K_tm_u + \left(R_4K_{tl} + M_2^2K_t + \frac{K_SK_D^2}{4L^2}\right)(m_s + m_u),$$

$$a_{44} = C_tM_3^2m_u - (m_s + m_u)\left(M_2^2C_t + \frac{C_SK_D^2}{4L^2}\right),$$

$$a_{45} = \frac{K_D(m_u + m_s)}{2L_S} \text{ and } a_{55} = -\frac{A_D}{\tau}$$

$$D = \frac{1}{A_D}\begin{bmatrix} 0 & 0\\ K_tm_uM_3^2 - M_1K_t & C_tm_uM_3^2 - M_1C_t\\ 0 & 0\\ K_tm_uM_3 - (m_s + m_u)M_3 & C_tm_uM_3 - (m_s + m_u)M_3\\ 0 & 0 \end{bmatrix}$$

$$B = \begin{bmatrix} 0\\ 0\\ 0\\ 0\\ \frac{1}{\tau} \end{bmatrix}$$

where,

$$M_1 = m_uP_5^2 + m_uP_8^2 + I_uP_2^2 + I_C,$$

$$M_2 = P_8 \text{ and, } R_4 = R_2^2 + 2R_1R_3$$

The parameters m_s, m_u, I_c, I_u, K_s, K_t, C_s, C_t and K_{tl} are sprung mass, unsprung mass, moment

Fig. 3 Photograph of MR damper

of inertia of the control arm and the wheel around the x-axis, stiffness of the Macpherson strut, stiffness of the tire, damping coefficient of strut and damping coefficient of tire and lateral stiffness of the tire respectively.

The cylindrical MR damper used in the present study is shown in Fig. 3. In the present study, a commercially available fluid, MRF 132-LD is used in the MR damper. The present study considers the damper model adopted by Choi et al.[8] as this model is found out to be suitable. The damping force of the MR damper is given by

$$F_D = K_e \Delta L + C_e \dot{\Delta L} + F_{MR}\, sign(\dot{\Delta L}) \tag{17}$$

where, K_e and C_e are the equivalent stiffness and damping coefficients of the MR damper which are considered to be equal to K_s and C_s. ΔL is the deflection of the MR damper and the force due to MR effect is given by

$$F_{MR} = (A_p - A_r)\frac{2L_p}{h_g}\alpha_1 H^{\alpha_2} \tag{18}$$

The coefficients l_p, H_g, A_p, A_r, α_1 and α_2 are length of the pole, annular gap, area of piston, area of piston rod and coefficients, respectively. H is the magnetic field obtained as, $H = \frac{NI}{2H_g}$, where N is the number of coil turns and I is the current.

3. Design of a New Controller

In this work, a moving sliding surface[9,10] is used instead of conventional fixed sliding surface defined by

$$\begin{aligned}\sigma &= c_1(x_1, x_2)x_1 + c_2x_2 + c_3x_3 + c_4x_4 \\ &\quad + c_5x_5 + \alpha m(x_1, x_2) \\ c_1(x_1, x_2) &= \frac{(\Delta_{rot} - x_2)}{x_1}, \\ \alpha_m(x_1, x_2) &= c_{10}x_1 + x_2 - \Delta_{sf}\end{aligned} \tag{19}$$

where, c_1, c_2, c_3, c_4, c_5 are surface gradients, c_{10} is the initial value of c_1 and Δ_{rot} and Δ_{sf} are the coefficients for rotating and shifting surfaces respectively. The moving sliding mode controller is defined as

$$\begin{aligned}u = -\frac{1}{CB}\{&CAx\ sgn(\sigma(x)) \\ &+ Ksgn(\sigma(x)) + \alpha_m(x_1, x_2)\}\end{aligned} \tag{20}$$

where, K is a discontinuous positive gain which is calculated as $|GDn|$, $n = [v_1 \ \ v_2]^T$ when $v_i > |w_i|$, for $i = 1,\ 2$. In order to handle three performance characteristics of vehicle suspension such as ride comfort, suspension travel, and road holding, the adaptation fuzzy logic based on the controller is designed and integrated with the sliding mode controller (20). The fuzzy rule is expressed as follows:

For inputs, **N** - Negative, **Z** - Zero, **P** - Positive.
For output, **ON** - One, **SP** - Small Positive.

The three rules are written as

IF $(a_s = P)$ OR $(x_{rel} = N)$ OR $(x_{20} = P)$
THEN $(u = ON)$.
IF $(a_s = N)$ OR $(x_{rel} = P)$ OR $(x_{20} = N)$
THEN $(u = ON)$.
IF $(a_s = Z)$ OR $(x_{rel} = Z)$ OR $(x_{20} = Z)$
THEN $(u = SP)$.

The control force is then given by

$$\begin{aligned}u = -(CB)^{-1}\{&CAx\ sgn(\sigma(x)) \\ &+ \tilde{\theta}K\ sgn(\sigma(x)) + \alpha_m(x_1, x_2)\}\end{aligned} \tag{21}$$

The stability of the controller (21) does not affect as $\tilde{\theta} > 1$ is always positive. We call it

AMSMC (adaptive moving sliding mode controller).

In order to compare the effectiveness of the proposed controller, the following two existing controllers are used.

1) Sky-Hook Controller

$$u = \begin{cases} u_{sky}, & \text{if } \dot{z}_s(\dot{z}_s - \dot{z}_u) > 0 \\ 0, & \text{otherwise} \end{cases} \quad (22)$$

where, u_{sky} is the damping force when the damper is at on state.

2) Conventional Sliding Mode Controller

$$u = -(CB)^{-1}\{CAx \ \ sgn(\sigma(x)) + K sgn(\sigma(x))\} \quad (23)$$

where, K is a discontinuous positive gain which is calculated as $|GDn|$, $n = [v_1 \ \ v_2]^T$ when $v_i > |w_i|$, for $i = 1,2$.

4. Results and Discussions

4.1 Bump Response

Control characteristics of the suspension system is measured for bump type transient road input which is given by

$$z_r - z_b[1 - \cos(\omega_r t)] \quad (24)$$

where, z_b is the half bump height (0.03 m), $\omega_r = 2\pi V / D_r$, D is the width of the bump (0.8 m) and V is the wheel velocity which is considered as 0.8 m/s (2.88 km/hr) in this study. The sprung mass displacement responses are plotted for different control algorithms in Fig. 4(a). The figure shows that all the control strategies perform better, where proposed control strategy provides better result. The figure also shows the settling time of the response which is found out to be 1.991s in AMSMC, reduced from 3.48 s for uncontrolled case. Settling time is calculated as the time for the system to reach within 20 % of the excitation amplitude. For the present case, the maximum input amplitude was 0.07 m. Thus, time required for the system to settle within 0.014 m in considered as settling time of the system. For sprung mass acceleration, the chattering is observed in sky-hook and sliding mode both cases, although sliding mode controller is used with saturation

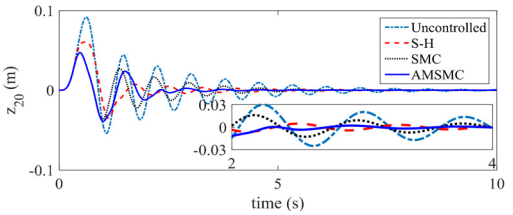

(a) Sprung mass deflection

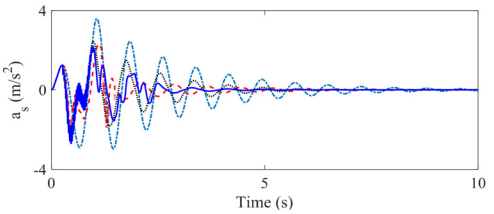

(b) Sprung mass acceleration

Fig. 4 Effect of different control strategies on the responses

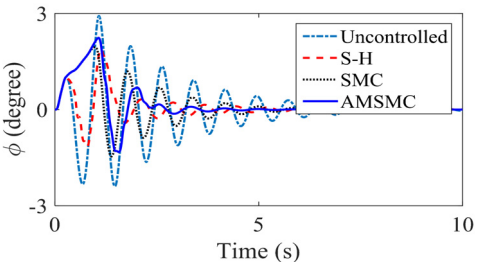

(a) Camber angle

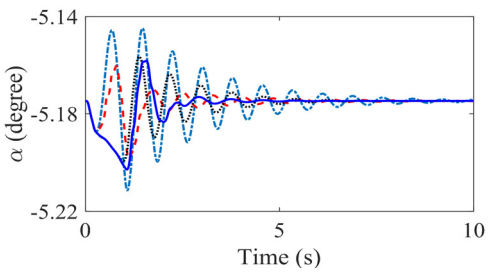

(b) King-pin angle

Fig. 5 Effect of different control strategies

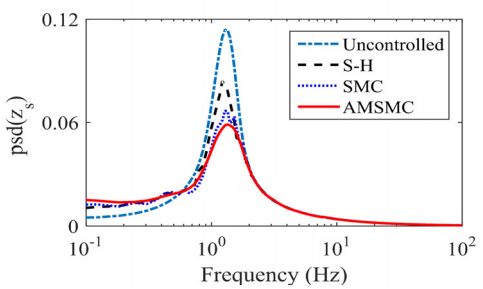

(a) Sprung mass displacement

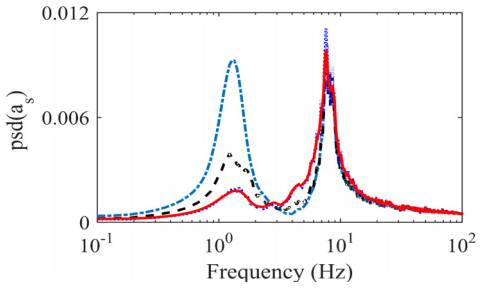

(b) Sprung mass acceleration

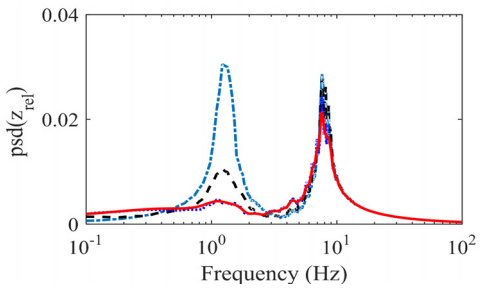

(c) Tire deflection

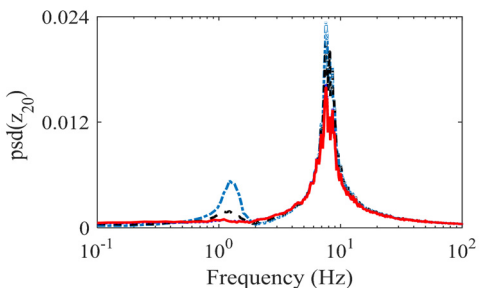

(d) Suspension travel

Fig. 6 Frequency response of the suspension system without parameter uncertainty

function (Fig. 4(b)). This may arise due to the semi-active control strategy applied. The important kinematic parameters like camber angle (φ), king-pin angle and track alteration are calculated and plotted in Fig. 5. Camber angle, which is plotted in Fig. 5(a), is shown to be improved and the response settled fast for the proposed control logic. The king-pin angle is the angle between the vertical axis in case of Macpherson strut and the line through the points A and D is calculated as

$$\alpha = \tan^{-1}\frac{y_D - y_A}{z_D - z_A} \tag{25}$$

The king-pin angle is plotted in Fig. 5(b) and it improves significantly when the proposed control logic is applied.

4.2 Random Response

Figure 6 represents the psd (power spectral density) of different performances in frequency domain for random excitation. The sprung mass displacement psd shows that the displacement reduced by a significant amount near the body resonance (1 Hz ~ 2 Hz).

From Fig. 6(b) it is seen that the sprung mass acceleration is also reduced near the body resonance frequency, but it worsen between body frequency and wheel frequency. This is due to the fact that in proposed control strategy, there is no acceleration term to be controlled. The tire deflection psd (Fig. 6(c)) is also reduced in both the body resonance and wheel resonances. The suspension travel is seen to be reduced by a good amount near both the resonances (Fig. 6(d)).

5. Conclusion

The stability of the vehicle depends on the strut parameters like camber angle, track alteration etc.

The nonlinear equations of motion obtained using Lagrangean formulation considering the dynamics of the system are linearized about a fixed point. To control of the motions of Macpherson strut a new adaptive moving sliding mode controller is proposed based on fuzzy logic. The results of proposed controller is compared with the

results obtained for ordinary sliding mode controller and for moving sliding mode controller for two types of input road disturbances, bump input and random road. The proposed control strategy is shown to improve the ride performances characteristics of the Macpherson strut like ride comfort, suspension travel and road handling. The proposed adaptive control makes the system to settle faster than the other control strategies.

References

(1) Karnopp, D., Crosby, M. J. and Harwood, R. A., 1974, Vibration Control Using Semi-active Force Generators, Journal of Manufacturing Science and Engineering, Vol. 96, No. 2, pp. 619~626.

(2) Ahmadian, M. and Vahdati, N., 2006, Transient Dynamics of Semiactive Suspensions with Hybrid Control, Journal of Intelligent Material Systems and Structures, Vol. 17, No. 2, pp. 145~153.

(3) Sung, K. G. and Choi, S. B., 2009, Vibration Control of Vehicle Suspension Featuring Magnetorheological Dampers: Road Test Evaluation, Transactions of the Korean Society for Noise and Vibration Engineering, Vol. 19, No. 3, pp. 235~242.

(4) Fallah, M. S., Bhat, R. and Xie, W. F., 2009, New Model and Simulation of Macpherson Suspension System for Ride Control Applications, Vehicle System Dynamics, Vol. 47, No. 2, pp. 195~220.

(5) Hurel, J., Mandow, A. and García-Cerezo, A., 2012, Nonlinear Two-dimensional Modeling of a McPherson Suspension for Kinematics and Dynamics Simulation, In Advanced Motion Control (AMC), 2012 12th IEEE International Workshop on IEEE, pp. 1~6.

(6) Hong, K. S., Jeon, D. S. and Sohn, H. C., 1999, A New Modeling of the Macpherson Suspension System and Its Optimal Pole-placement Control, In Proceedings of the 7th Mediterranean Conference on Control and Automation, pp. 28~30.

(7) Andersen, E. R., 2007, Multibody Dynamics Modeling and System Identification for a Quarter-car Test Rig with McPherson Strut Suspension, Doctoral dissertation, Virginia Polytechnic Institute and State University.

(8) Choi, S. B., Choi, Y. T., Chang, E. G., Han, S. J. and Kim, C. S., 1998, Control Characteristics of a Continuously Variable ER Damper, Mechatronics, Vol. 8, No. 2, pp. 143~161.

(9) Choi, S. B., Park, D. W. and Jayasuriya, S., 1994, A Time-varying Sliding Surface for Fast and Robust Tracking Control of Second-order Uncertain Systems, Automatica, Vol. 30, No. 5, pp. 899~904.

(10) Choi, S. B., Cheong, C. C. and Park, D. W., 1993, Moving Switching Surfaces for Robust Control of Second-order Variable Structure Systems, International Journal of Control, Vol. 58, No. 1, pp. 229~245.

Seung-Bok Choi received the B.S. degree in Mechanical Engineering from Inha University in 1979, MS degree and Ph.D. degrees from Michigan State University in 1986 and 1990, respectively. He is currently Dean of the Graduate School and fellow professor in Inha University. He is a fellow of NAEK(National Academy Engineering of Korea), KAST(The Korean Academy of Science and Technology). His research interests are robust controller design and control of various systems using smart actuators.